Journal of Inorganic Biochemistry 203 (2020) 110915

Contents lists available at ScienceDirect

Journal of Inorganic Biochemistry

journal homepage: www.elsevier.com/locate/jinorgbio

The interaction of aluminium-based adjuvants with THP-1 macrophages in vitro: Implications for cellular survival and systemic translocation

Emma Shardlow, Matthew Mold, Christopher Exley*

The Birchall Centre, Lennard-Jones Laboratories, Keele University, Keele, Staffordshire ST5 5BG, UK

ARTICLE INFO

Keywords:
Aluminium-based adjuvants
Vaccination
THP-1 macrophages
Phagocytosis
Cell survival

ABSTRACT

Within clinical vaccinations, recombinant antigens are routinely entrapped inside or adsorbed onto the surface of aluminium salts in order to increase their immunological potency in vivo. The efficacy of these immunisations is highly dependent upon the recognition and uptake of these complexes by professional phagocytes and their subsequent delivery to the draining lymph nodes for further immunological processing. While monocytes have been shown to internalise aluminium adjuvants and their adsorbates, the role of macrophages in this respect has not been fully established. Furthermore, this study explored the interaction of THP-1 macrophages with aluminium-based adjuvants (ABAs) and how this relationship influenced the survival of such cells in vitro. THP-1 macrophages were exposed to low concentrations of ABAs (1.7 μg/mL Al) for a maximum of seven days. ABA uptake was determined using lumogallion staining and cell viability by both DAPI (4′,6-diamidino-2-phenylindole) staining and LDH (lactate dehydrogenase) assay. Evidence of ABA particle loading was identified within cells at early junctures following treatment and appeared to be quite prolific (> 90% cells positive for Al signal after 24 h). Total sample viability (% LDH release) in treated samples was predominantly similar to untreated cells and low levels of cellular death were consistently observed in populations positive for Al uptake. It can thus be concluded that aluminium salts can persist for some time within the intracellular environment of these cells without adversely affecting their viability. These results imply that macrophages may play a role in the systemic translocation of ABAs once administered in the form of an inoculation.

1. Introduction

In order to increase both the longevity and potency of the immunological response incurred post immunisation, formulations containing recombinant antigens are often supplemented with aluminium salts. These immunopotentiating compounds are physicochemically distinct and include aluminium oxyhydroxide (AH), aluminium hydroxyphosphate (AP) and the recently introduced proprietary suspension aluminium hydroxyphosphate sulphate (AAHS). Such materials remain the archetypal choice of adjuvant included within clinically-approved vaccinations and are considered highly efficacious with regards to the generation of humoral/antibody mediated immunity (see reviews [1,2]). However, their ability to induce Th1 responses appears to be severely restricted [3–6] and as such precludes their inclusion within inoculations designed to target pathogens where a cell-mediated counterstrike is required. Concerns have also been expressed regarding the safety of these adjuvants, most notably the emergence of macrophagic myofasciitis (MMF), a disease attributed to the chronic intramuscular influx of periodic acid–Schiff-positive antigen-presenting cells (APCs) in predisposed individuals following AH administration [7–10].

The biological fate of aluminium-based adjuvant (ABA) particles once introduced by means of vaccination into the interstitial milieu continues to be the source of some debate. Current consensus suggests that a proportion of the aluminium injected remains localised at the injection site for extended periods of time. Indeed, the cumulative absorption of AH & AP into the bloodstream is substantially impeded due to their diminutive dissolution rates under simulated in vivo conditions [11,12] and equated to 17 & 51% respectively over a period of 28 days [12,13]. Consistent with such observations, immunisation of primates against diphtheria-tetanus induced the formation of localised aluminium-rich granulomas/nodules, which could endure for up to 12 months post inoculation [14]. Munks et al. concluded that similar nodules formed following intraperitoneal injection consisted predominantly of fibrin and due to the concomitant presence of histones bore a striking resemblance to extracellular traps (ETs); however, these pathological hallmarks were deemed redundant with regards to the adjuvanticity of aluminium salts [15]. Such phenomena were also

* Corresponding author.
E-mail address: c.exley@keele.ac.uk (C. Exley).

https://doi.org/10.1016/j.jinorgbio.2019.110915
Received 30 August 2019; Received in revised form 31 October 2019; Accepted 8 November 2019
Available online 12 November 2019

observed subcutaneously at early junctures post vaccination, although these were typically rich in neutrophilic activity and provided an abundant source of extracellular DNA through NETosis associated mechanisms, which subsequently enhanced the production of ovalbumin-specific IgG1 [16]. While the formation of an antigen depot is generally considered dispensable in relation to the adjuvant activity of aluminium salts [17], it is possible that these structures may contribute to the *modus operandi* of these compounds through the generation of localised damage-associated molecular patterns (DAMPs), whose release is known to facilitate the recruitment of leukocytes towards sites of physiological insult [18,19].

Furthermore, the development of robust adaptive immune responses post vaccination is highly dependent upon the successful translocation of antigenic material, presumably as part of an antigen-adjuvant complex, to the draining lymph nodes for immunological processing [20]. While the large hydrodynamic size of ABAs in biological fluid stymies the chances of independent migration [21], their micron- sized dimensions expedite their recognition and uptake by professional phagocytes [22], the presence of which is observed at the site of injection as early as 2 h post inoculation [23]. Monocytes, in particular, have a voracious appetite for aluminium salts [21,24,25] which in turn provides a potent stimulus for their differentiation into a mature dendritic phenotype [26–28]. These specialised APCs are responsible for much of the antigen-presentation and processing observed following vaccine administration [29] and thus play a pivotal role in the immunomodulatory events directed by ABAs [29–32].

A tentative role for macrophages in these proceedings has also been postulated, despite their seemingly superfluous contribution to murine T-cell priming and antibody generation following immunisation with AH [33]. The direct interaction of AH with tissue-resident macrophages promotes leukocyte chemotaxis [27] and induces alterations in surface marker expression towards that typically associated with dendritic cells [34,35]. While some reports suggest that AH microparticles are not engulfed by macrophages in vitro [36,37], others have indicated that monocyte-derived macrophages internalise ABAs present in both the intramuscular [38] and subcutaneous cavities in vivo [39]. These cells are then capable of disseminating their cargo throughout the body to myriad locations including the spleen, lymphatic nodes and brain [38–41]. The extent or likelihood of systemic translocation is expected to be governed by the ability of loaded macrophages to survive for extended periods of time post particulate uptake. Preliminary research has indicated that ABAs can promote DNA synthesis in bone-marrow derived macrophages (BDMCs) which enhances cellular endurance [42]; however, this short-term study did not explicitly follow ABA uptake/recognition in conjunction with viability. In order to determine the survival prospects of APCs in the presence of ABAs, this study monitored the direct interaction of THP-1 macrophages with low doses of clinically relevant ABAs in tandem with their viability for one week post initial exposure.

2. Materials and methods

2.1. Adjuvants

Aluminium oxyhydroxide (Alhydrogel® 2%) and aluminium hydroxyphosphate (Adju-Phos®) were obtained from Brenntag Biosector, Denmark as aseptic colloidal suspensions containing a total aluminium (Al) concentration of *ca* 10 and 5 mg/mL respectively. Pyrogenicity testing was performed by the manufacturer and endotoxin levels were certified as within acceptable limits.

2.2. Cell culture protocols

2.2.1. Maintenance of THP-1 parent cultures

Growing cultures of THP-1 cells (ECACC 88081201), a line originally isolated from the blood of a paediatric patient suffering from acute monocytic leukaemia [43], were obtained from Public health England (PHE). Parent cultures were maintained in Corning® T25 flasks at a density of 5×10^5–8×10^5 cells/mL within GlutaMAX™ RPMI 1640 medium supplemented with an additional 20 μg/mL gentamycin and 10% foetal bovine serum (R10 medium). Flasks were housed under humidified conditions at 37 °C, 5% CO_2.

2.2.2. THP-1 differentiation and treatment

Prior to differentiation, the viability of cells isolated from parent cultures was determined using a trypan blue exclusion test. Provided that the viability of enumerated monocytes exceeded 90%, cells were seeded into 24- or 96-well plates at a density of 2×10^5 and 2×10^4 cells per well respectively and differentiated using 50 nM PMA (phorbol 12-myristate 13-acetate) for 48 h (37 °C, 5% CO_2). Cells in 24-well plates were differentiated onto 13 mm round coverslips, which had previously been sanitised using 70% v/v EtOH. Following differentiation, the PMA-containing medium was removed and replaced with fresh R10 medium in which cells were allowed to rest under the same environmental conditions for a further 24 or 48 h depending on the intended purpose of proceeding experiments.

2.2.3. ABA treatment of THP-1 macrophages

ABA formulations containing *ca* 300 μg/mL Al were initially prepared through the addition of adjuvant stock solutions to physiological saline (0.9% NaCl, pH 7, 0.22 μm filtered). These solutions were further diluted in R10 medium to a concentration of 1.7 μg/mL Al before replacing the resting medium originally residing in wells designated for adjuvant treatment. Cells were treated on day 2 of the rest period following differentiation and incubated at 37 °C (5% CO_2) for the duration of the experimental procedure. Macrophages were analysed on days 1, 3 & 7 post adjuvant exposure, which corresponded to days 3, 5 & 9 post PMA withdrawal. For preliminary uptake experiments using fixed cells, samples were also analysed 3 h after treatment with ABAs.

2.3. Lumogallion staining (Al detection)

Macrophagic interaction with ABAs was monitored using lumogallion staining, a highly sensitive ligand for aluminium [44] which emits a fluorescence signal at *ca* 590 nm upon complexation with the ionic form of the metal [45]. The following protocol was adapted from that used by Mold et al. [25] for the purpose of labelling native THP-1 monocytes in vitro.

A stock solution of lumogallion (1 mM, Sigma Aldrich, UK) was prepared in ultrapure water (0.067 μS/cm) and filtered using a sterile 0.22 μm membrane in order to remove potential microbial or particulate contamination. Both adjuvant-treated and control wells were spiked with 20 μL of the stock solution (final concentration - 100 μM per well) 2 h prior to fixation or DAPI staining of live cells.

2.4. Dead cell labelling and detection (live cell staining)

Labelling of nuclear material through DAPI staining of live cell populations was used in order to determine the relative number of membrane-compromised macrophages per treatment.

DAPI (4′,6-diamidino-2-phenylindole, dihydrochloride) was procured from Thermo Fisher Scientific, UK and stock aliquots (5 mg/mL) were prepared through dissolution of the powder in ultrapure water (0.22 μm filtered). Aliquots were serially diluted prior to experimental use first in ultrapure water (1:100) and then in 1X Dulbecco's phosphate-buffered saline (DPBS) ($+Ca^{2+}$ and Mg^{2+}) (1:500) to achieve a final working concentration of 0.1 μg/mL.

ABA-treated and control cells were washed once with warm 1X DPBS ($+Ca^{2+}$ and Mg^{2+}) before the addition of 100 μL dilute DAPI stain to wells and thereafter incubated at RT for 15 min in the absence of light. Post incubation, macrophages were washed once more to remove excess DAPI stain and analysed immediately using fluorescence microscopy.

2.5. Fixation procedure

Cells cultured in 24-well plates were washed once with warm 1X DPBS ($+Ca^{2+}$ and Mg^{2+}) and fixed for 20 min at RT using sterile filtered paraformaldehyde (4% w/v in 0.9% NaCl + 25 mM PIPES (piperazine-*N*,*N*′-bis(2-ethanesulfonic acid)), pH 7.4). Following a further two washes with 1X DPBS (-Ca^{2+} and Mg^{2+}), coverslips were mounted onto slides using a small amount of DAPI containing ProLong® Gold Antifade Reagent (Life technologies, UK) and were allowed to rest for 24 h at 4 °C prior to analysis by fluorescence microscopy.

2.6. Fluorescence microscopy (fixed cells)

The time-dependent interaction of ABA particles with THP-1 macrophages over an initial period of 2 days was monitored using a BX50 fluorescence microscope (Olympus, UK) fitted with a BX-FLA reflected fluorescent light attachment (mercury source) and a vertical illuminator.

Lumogallion fluorescence emanating from Al positive material (orange signal) was detected through the use of an Olympus U-MNIB3 fluorescence filter cube (λ_{ex}: 470 –495 nm, dichromatic mirror: 505 nm, longpass λ_{em}: 510 nm).

DAPI fluorescence originating from labelled cell nuclei (blue signal) was observed using an Olympus U-MWU2 fluorescence filter cube (λ_{ex}: 330–385 nm, dichromatic mirror: 400 nm, longpass λ_{em}: 420 nm). Images were acquired using a ColorView III CCD camera using the Cell D software suite (Olympus, Soft Imaging Solutions, SiS, GmbH, Münster, Germany).

2.7. Light and fluorescence microscopy (live cell imaging)

The impact of ABAs upon the viability of macrophages in live culture was determined directly in plate wells using an EVOS FL cell imaging system equipped with an LED light source (Thermo Fisher Scientific, UK).

The location of ABA particles (red lumogallion fluorescence) was visualised using the RFP fluorescence channel (filter cube λ_{ex} & λ_{em}: 531–540 nm and 593–640 nm respectively).

Positively stained extracellular and intracellular nuclear material originating from membrane compromised cells (blue DAPI fluorescence) was detected using the DAPI fluorescence channel (filter cube λ_{ex} & λ_{em}: 357–444 nm and 447–560 nm respectively).

The size (diameter) of native and differentiated THP-1 cells was obtained using the measurement tools available within Cell D software suite (Olympus, UK).

2.8. Lactate dehydrogenase (LDH) assay

As a general indicator of cell death, the release of lactate dehydrogenase (LDH) by THP-1 macrophages was monitored using a commercially available assay kit (Pierce, Thermo Scientific, UK) according to the manufacturer's instructions.

Negative assay controls in the absence of cells included R10 medium only (med) in addition to medium spiked with ABAs (med ABA) (1.7 μg/mL Al). The latter was included in order to determine whether ABAs themselves had the potential to interfere directly with the assay results.

Maximum LDH release values (positive controls) were obtained via pre-treatment of designated wells with 10 μL lysis buffer (10% v/v per well) for 45 min (37 °C, 5% CO_2). The potential for LDH adsorption onto the surface of ABAs also prompted the introduction of supplementary ABA-containing positive controls (max ABA) (1.7 μg/mL Al).

Briefly, a small amount of supernatant (50 μL) from treated and control wells was removed and transferred to a new 96-well plate. An equivalent volume of LDH reaction solution was added to each sample and the plate was incubated at RT for 30 min in the absence of light to allow colour development. The amount of LDH within each supernatant was derived from the enzyme-mediated reduction of INT to formazan which was measured at Abs 490 nm (680 nm background correction) using a TECAN M200 infinite pro plate reader. Mean absorbance values per condition were derived from the values obtained across triplicate wells provided that RSD < 10%. The % LDH released by untreated (un) and treated cells (t) was calculated in accordance with Eqs. (1) & (2) respectively:

$$(([A]_{un} - [A]_{med})/([A]_{max} - [A]_{med})) \times 100 \quad (1)$$

$$(([A]_{t} - [A]_{med\ ABA})/([A]_{max\ ABA} - [A]_{med\ ABA})) \times 100 \quad (2)$$

2.9. Statistical analyses

Statistical significance was determined using GraphPad Prism v.7 software and dataset normality was determined using a Shapiro-Wilk test before subsequent comparisons were conducted. Differences in size distribution parameters were analysed using a Friedman test followed by Dunn-post hoc tests. Time-dependent multiple comparisons were performed using a one or two-way ANOVA with repeated measures followed by Tukey or Sidak's post-hoc tests respectively. Multiple independent comparisons were performed using an ordinary one-way ANOVA followed by Tukey post hoc tests. Statistical significance was confirmed when a comparison yielded a P value of ≤ 0.05.

3. Results

3.1. Validation of differentiation protocol

In lieu of traditional immunocytochemical staining for markers of THP-1 differentiation including CD14 and CD11b, the success of the PMA-mediated differentiation procedure was determined through visual assessment of morphological changes to cells.

Native THP-1 monocytes (Fig. 1A) presented as a homogenous population of predominantly spherical entities ranging from 10.2–20.3 μm in size (d50–12.1 μm, Fig. 1D), which on occasion exhibited evidence of sparsely distributed granules within their cytoplasmic space. Following PMA withdrawal, cells became generally more heterogenous with respect to cytoplasmic volume, morphology and granularity (Fig. 1B & C). The former was characterised by a significant elevation in the overall breadth of the size distribution obtained and increase in the median size of cells (8.4–65.2 μm and 21.0 μm respectively, $P = 0.0002$), trends which remained consistent on the second day of analysis (11.7–100.7 μm and 20.9 μm respectively, $P = 0.59$). Extensive cellular elongation, adherence and generation of pseudopodia were also frequently observed along with heightened incidence of granule formation within the intracellular environment.

3.2. Survival of THP-1 macrophages post PMA withdrawal

In order to determine the maximum duration over which cells remained viable in vitro and thus could be monitored in the presence of ABAs, the membrane integrity of THP-1 macrophages was determined over a period of 9 days post PMA withdrawal.

Bereft of medium replenishment, the percentage of macrophagic LDH discharged into the extracellular environment was consistently low over the first 3 days, accounting for between 6.9 ± 4.9 and 9.0 ± 3.3% of the maximum sample recovery ($P = 1$) (Fig. 2 – purple series). The amount of LDH released by cells increased to 29.1 ± 5.6% after 5 days; however, this increase in value was not statistically significant with respect to that obtained for the previous time point ($P = 0.14$). By the end of the experiment (day 8), enzymatic release had burgeoned substantially to 53.8 ± 10.6% indicating that below half the population of macrophages in culture remained viable under these conditions.

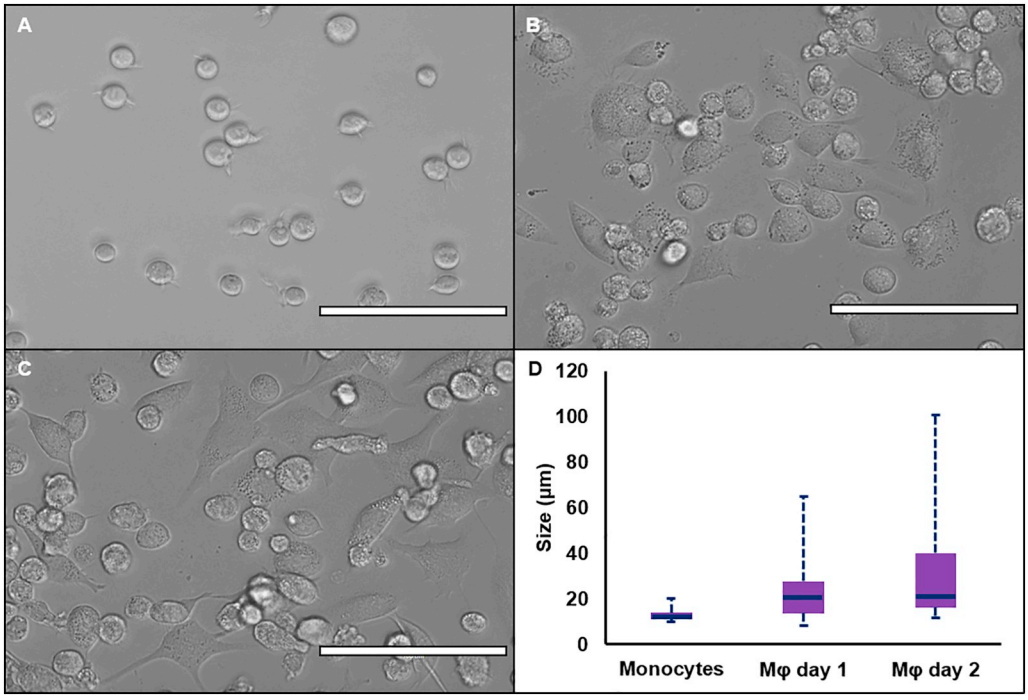

Fig. 1. Morphological characteristics of THP-1 monocytes exposed to 50 nM PMA for 15 min (A) and post withdrawal (24 and 48 h – panel B & C respectively). Images were taken on brightfield channel at a magnification of 400× and scale bars represent 100 µm. Panel D shows the size distribution of cells obtained at each time point as derived from $n = 30$ individual measurements. Blue dotted lines represent the span of the distribution whereas the interquartile range and d50 values are highlighted by purple boxes and blue lines respectively.

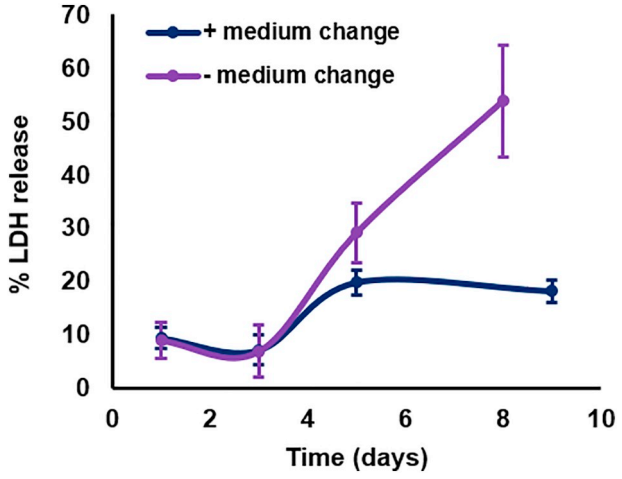

Fig. 2. Viability of THP-1 macrophages over a maximum of 9 days post differentiation (50 nM PMA for 48 h). Data shows the % LDH release of untreated macrophages relative to that obtained for respective positive controls (max. LDH release). The purple data series represents values obtained for cells where no medium change was conducted while those highlighted in blue were subject to medium replenishment every three days. Error bars represent ± SD of the measurement where $n = 3$. (For interpretation of the references to colour in this figure legend, the reader is referred to the web version of this article.)

Taking these results into consideration, similar experiments were performed with the inclusion of a medium replacement every three days, in order to assess whether this latter heightened cell death was due to nutrient depletion and thus could be ameliorated (Fig. 2 – blue series). Following the first medium change, the amount of LDH released by day 5 had decreased relative to that measured in the absence of nutrient replenishment (19.8 ± 2.3 vs. 29.1 ± 5.6%, $P = 0.006$) and appeared to plateau at moderate levels thereafter (Day 9 - 18.2 ± 2.1%).

3.3. Macrophagic loading of ABA particles following short term exposure

To optimise the adjuvant exposure protocol and maximise the amount of intracellular particulate loading prior to viability measurements, the interaction of Alhydrogel® (Alh) (1.7 µg/mL Al) with differentiated macrophages was monitored using lumogallion over the course of two days (Fig. 3).

The cytosol of control macrophages stained with lumogallion in the absence of ABAs emitted an extremely weak, orange autofluorescence signal and DAPI positive fluorescence (blue) confirmed the presence of multiple intact and regular nuclei (Fig. 3A). Following initial 3 h treatment with Alh (Fig. 3B), intense punctate orange fluorescence was detected both in the extracellular environment and intracellular compartment of cells as well as surrounding their membrane boundary. Particulate internalisation appeared to increase with contact time resulting in an extensive depletion of adjuvant from the culture medium 24 h post exposure and beyond (Fig. 3C & D). As a consequence, heightened cytoplasmic loading was frequently observed, although this was slightly more pronounced in samples treated for 24 h.

3.4. Survival of THP-1 macrophages treated with ABAs – day 1

In light of the results obtained for macrophage survival and ABA uptake, the survival of macrophages in the presence of ABAs (1.7 µg/mL Al) was analysed over a period of 7 days following treatment, which occurred on day 2 post PMA withdrawal.

After 24 h exposure to ABA particles, intense red lumogallion fluorescence was typically observed both within membrane boundaries and the surrounding peripheries of macrophages treated with Alh and Adju-Phos® (Adj) (Fig. 4B & C, respectively) in comparison to control cells, which demonstrated no appreciable lumogallion signal (Fig. 4A). Cellular loading appeared heterogenous in nature, varying between cytosolic saturation and limited incidence of intracellular particulates. However, the majority of cells sampled appear to exhibit some degree of intracellular or peripheral lumogallion fluorescence with limited differences in the former visualised between Adj treatments vs. those spiked with Alh (91.8 ± 5.8 vs. 90.5 ± 1.8%) (Table 1). Furthermore, only a few of these cells demonstrated DAPI positive nuclear staining indicating that a high percentage remained viable under these conditions (9.9 ± 6.5 & 5.5 ± 0.5% respectively).

The amount of LDH released by Alh-treated macrophages also remained low and did not deviate significantly from that observed in their untreated counterparts (11.1 ± 1.7 vs. 7.2 ± 2.7%, $P = 0.67$) (Fig. 4D).

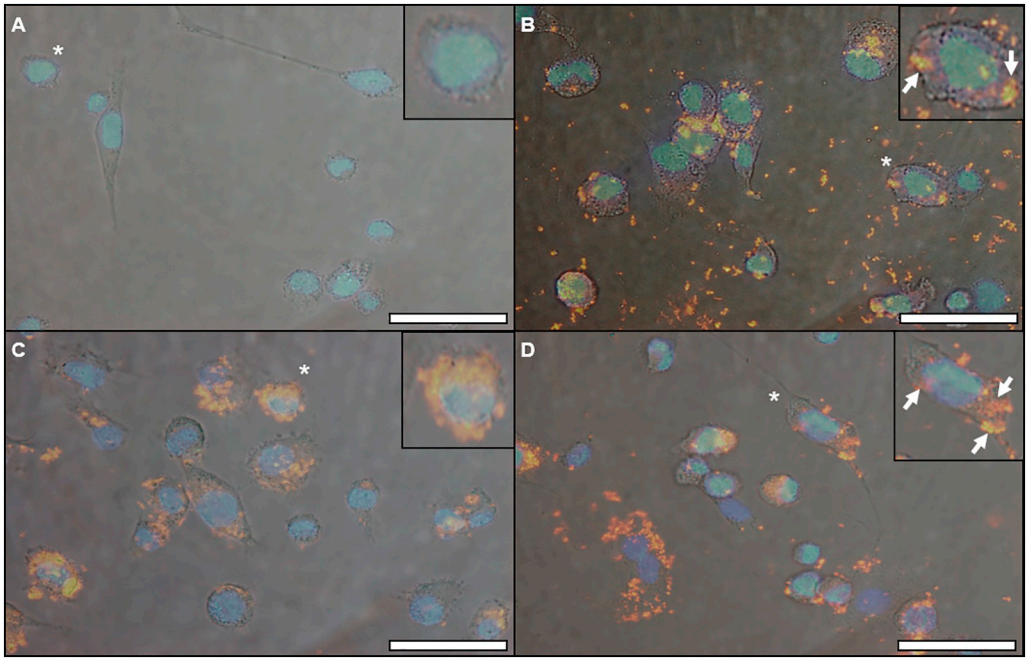

Fig. 3. Brightfield, lumogallion (NIB) and DAPI (WU) overlay images of THP-1 macrophages exposed to Alh (1.7 μg/mL Al). Panel A shows untreated cells 24 h post PMA withdrawal while panels B, C & D represent cells in the presence of adjuvant 3, 24 & 48 h post treatment respectively. Images were taken at a final magnification of 400× and scale bars represent 50 μm. Cells pictured in magnified inserts are identified by an asterisk and arrows highlight internalised aluminium particles.

Nevertheless, Adj did facilitate a significant elevation in total enzymatic discharge vs. the control (16.0 ± 1.0 vs. 7.2 ± 2.7%, $P = 0.03$), although no difference in release was observed between adjuvant groups ($P = 0.07$).

3.5. Survival of THP-1 macrophages treated with ABAs – Day 3

ABA particles continued to persist within the intracellular compartment of THP-1 macrophages 3 days following treatment (Figs. 5B & C). Patterns of loading and the number of aluminium positive cells were similar to that observed on day 1 with the latter accounting for 93.8 ± 3.6 & 88.5 ± 8.8% of the population surveyed (Alh and Adj respectively). Of these cells only 8.6 ± 4.4 & 10.1 ± 5.9% exhibited nuclei labelled by DAPI staining.

LDH levels in the extracellular environment of untreated cells increased relative to those detected on day 1 of the experiment (19.8 ± 2.3 vs.7.2 ± 2.7%, $P = 0.0008$) as did those observed in both adjuvant treatments (Alh and Adj – 26.7 ± 0.4 & 28.5 ± 5.2%, $P = 0.0003$ & 0.002 respectively) (Fig. 7). The presence of ABA particles, however, did not appear to accelerate LDH release in comparison to untreated cells ($P = 0.31$ & 0.23 respectively) nor did the species of adjuvant administered ($P = 0.96$) (Fig. 5D).

3.6. Survival of THP-1 macrophages treated with ABAs – day 7

By day 7, a substantial proportion of cells appeared to have reverted to a rounded morphology reminiscent of native THP-1 cells (de-

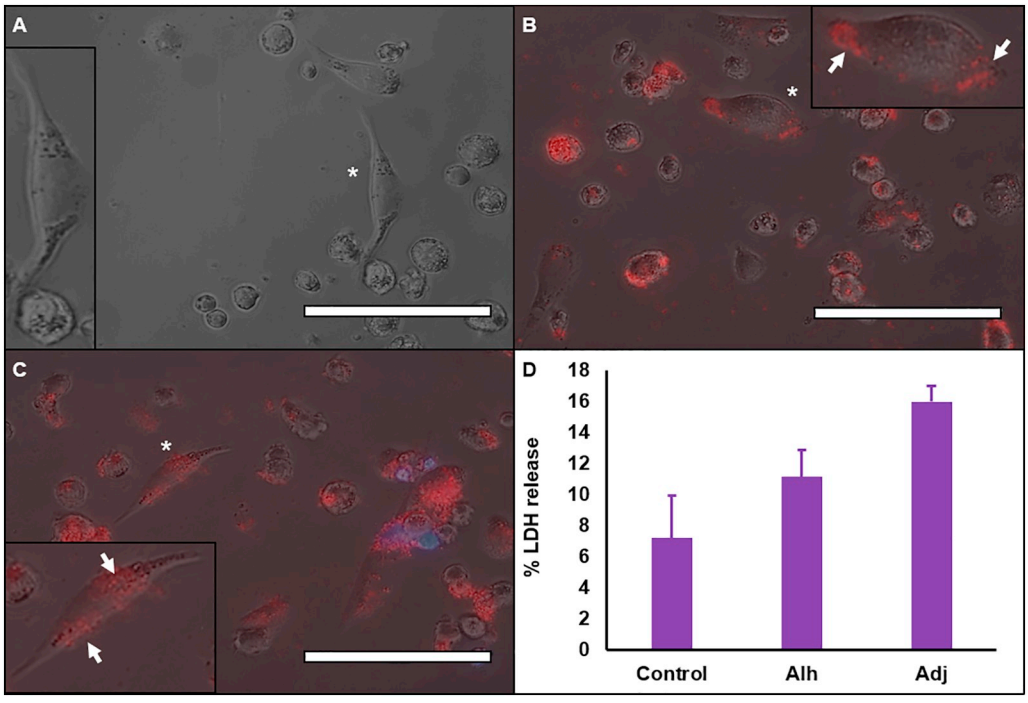

Fig. 4. Brightfield, phase contrast, lumogallion (RFP) and DAPI (WU) overlay images of THP-1 macrophages exposed to ABA particles (1.7 μg/mL Al) for 24 h. Panel A shows untreated cells 3 days post PMA withdrawal while panels B & C represent cells in the presence of Alh and Adj on day 1 post treatment respectively. Images were taken at a final magnification of 400× and scale bars represent 100 μm. Cells pictured in magnified inserts are identified by an asterisk and arrows highlight internalised aluminium particles. Panel D shows the LDH release (%) induced by each condition relative to that obtained for respective positive controls (max. LDH release). Error bars represent ± SD of the measurement where $n = 3$.

Table 1
Percentage of cells exhibiting evidence of Al internalisation or association and the percentage of Al positive cells which appeared to be dead (DAPI positive nuclei). Data for each condition was derived from counts obtained from three independent representative images taken at 200× magnification (see Figs. S2–4 for examples of such images).

Time post treatment (days)	Al positive cells (% ± SD)	Al positive dead/dying cells (% ± SD)
Alh		
1	90.5 ± 1.8	5.5 ± 0.5
3	93.8 ± 3.6	8.6 ± 4.4
7	57.1 ± 11.7	8.1 ± 7.1
Adj		
1	91.8 ± 5.8	9.9 ± 6.5
3	88.5 ± 8.8	10.1 ± 5.9
7	61.4 ± 5.5	3.2 ± 2.0

differentiation); however, a few macrophage-like entities did persist and cellular adherence remained satisfactory (Fig. 6A). While loading remained intensive within a small proportion of cells (Fig. 6B & C), the number of cells expressing a positive signal for Al decreased to 57.1 ± 11.7 and 61.4 ± 5.5% (Alh and Adj, respectively). The number of labelled nuclei witnessed within such populations accounted for 8.1 ± 7.1 and 3.2 ± 2.0%, the latter being substantially smaller than that observed on day 3.

LDH release appeared to plateau under all conditions in relation to that measured on the previous time point (Control, Alh & Adj - 18.2 ± 2.1, 26.9 ± 4.9 & 30.5 ± 1.3%, $P = 0.13$, 0.75 & 0.06 respectively). Variations between ABA treated and untreated groups were also inconsequential at this stage (Alh & Adj vs. control - $P = 0.51$ & 0.15 respectively) as were those observed amongst different adjuvant treatments ($P = 0.60$) (Fig. 6D).

4. Discussion

Our data have revealed, for the first time, that THP-1 macrophages can survive for extended periods in vitro despite significant intracellular burdens of ABAs. Given that the amount of Al encountered at the injection site can be substantial (up to 0.85 mg/dose if the Al concentration of the vaccine is determined by assay [46]), we are aware that our use of such low doses of ABAs, in this case 1.7 μg/mL, may be considered a potential caveat of this research. However, this study was not intended to mimic the in vivo concentration of Al administered at the injection site but rather to establish if: i) ABAs could be internalised/recognised by THP-1 macrophages and ii) to determine if the presence of cytosolic Al was directly responsible for cell death and thus impacted the long-term survival of these cells. At higher concentrations of Al (12.5 μg/mL) cells were often masked by the swathe of inorganic material, which impeded the direct visualisation of such events (data not shown). Therefore, in order to definitively achieve our aims, an optimised and very low dose of Al had to be applied.

In an attempt to elucidate the impact of ABAs upon the survival of macrophages in vitro, the studies performed in this work employed the use of cells differentiated from a malignant monocytic precursor (THP-1), which possess a similar phenotype to primary cells from a similar lineage [47–51]. The phagocytic capacity of these cells for inorganic particles is also similar to that of monocyte-derived macrophages (MDMs) provided that both the rest period and contact time with the differentiating agent are sufficient [47,52]. Initial experiments indicated that exposure to increasing concentrations of PMA (100 nM max.) did not adversely impact the longevity of THP-1 macrophages relative to the application of lower concentrations (Fig. S1). However, cellular survival was prolonged and overall death reduced through the application of medium changes every three days. While our study did not use the lowest recommended concentration of PMA required to induce stable differentiation of THP-1 cells, levels of adherence following long-term withdrawal (5 days) were reportedly higher in populations differentiated with higher doses of PMA [50]. This provides a substantial advantage in terms of being able to monitor such cells over extended periods and thus a concentration of 50 nM was selected for use in active experiments. Nevertheless, care must be taken when using high concentrations of differentiating agents as cellular responses to pathogenic stimuli, in particular, can deviate substantially from those of MDMs [51]. Limitations of this model also include the tendency of differentiated cells to revert to a monocytic phenotype approximately one week following PMA removal (Fig. 6A), which may lead to an alteration in their response to ABAs at latter experimental junctures. Given the propensity of native THP-1 cells to proliferate in vitro, it is

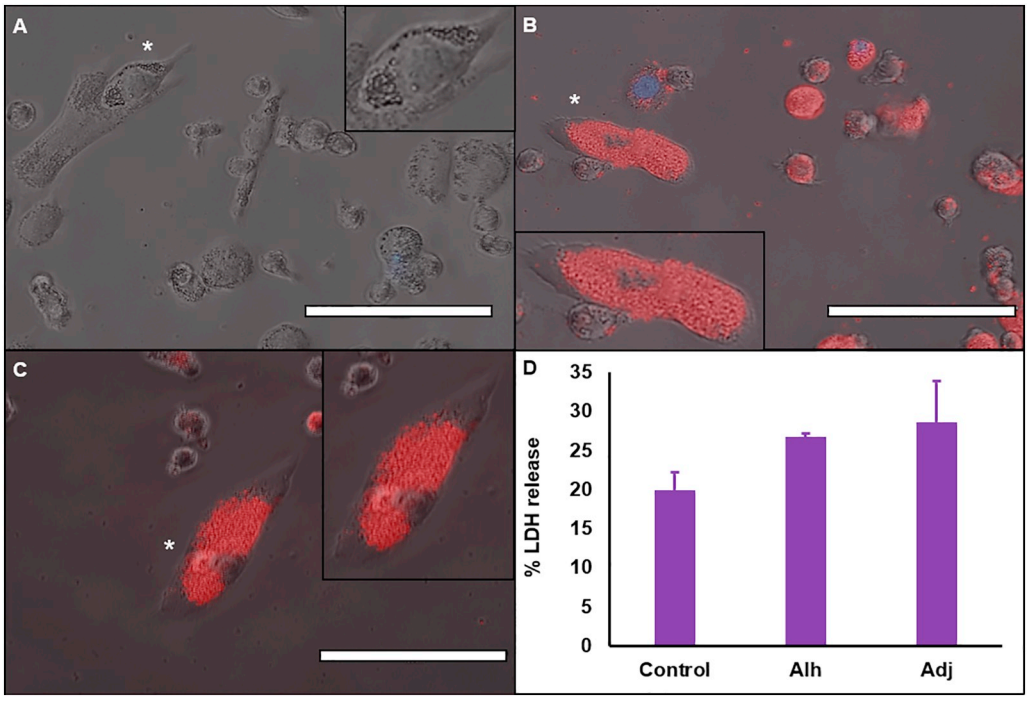

Fig. 5. Brightfield, phase contrast, lumogallion (RFP) and DAPI (WU) overlay images of THP-1 macrophages exposed to ABA particles (1.7 μg/mL Al) for 3 days. Panel A shows untreated cells 5 days post PMA withdrawal while panels B & C represent cells in the presence of Alh and Adj on day 3 post treatment respectively. Images were taken at a final magnification of 400× and scale bars represent 100 μm. Cells pictured in magnified inserts are identified by an asterisk. Panel D shows the LDH release (%) induced by each condition relative to that obtained for respective positive controls (max. LDH release). Error bars represent ± SD of the measurement where $n = 3$.

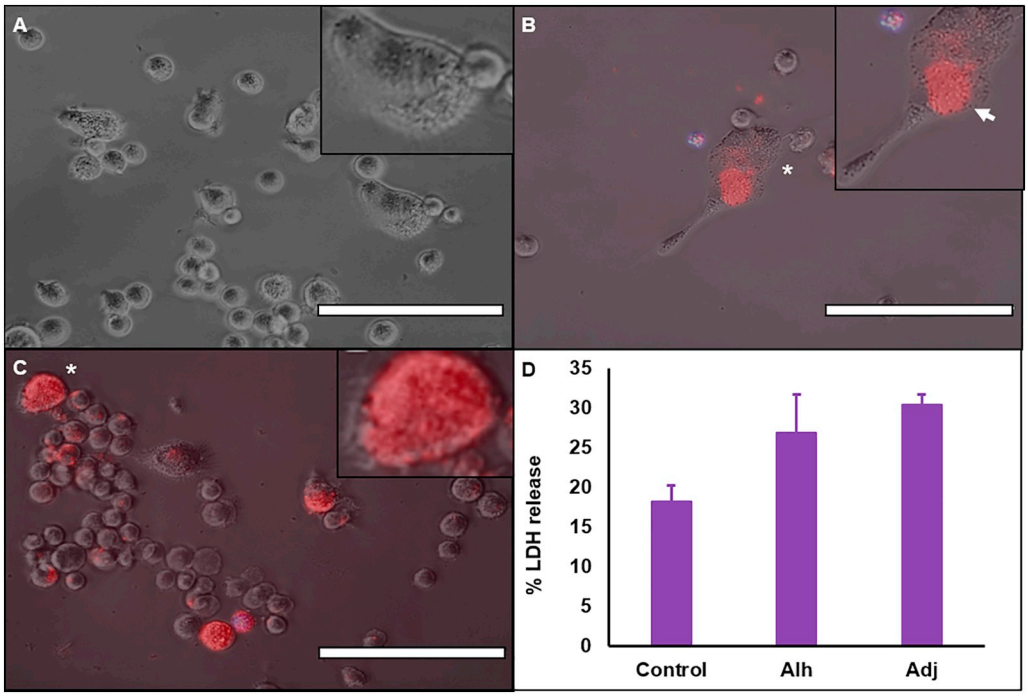

Fig. 6. Brightfield, phase contrast, lumogallion (RFP) and DAPI (WU) overlay images of THP-1 macrophages exposed to ABA particles (1.7 μg/mL Al) for 1 week. Panel A shows untreated cells 9 days post PMA withdrawal while panels B & C represent cells in the presence of Alh and Adj on day 7 post treatment respectively. Images were taken at a final magnification of 400× and scale bars represent 100 μm. Cells pictured in magnified inserts are identified by an asterisk and arrows highlight internalised aluminium particles. Panel D shows the LDH release (%) induced by each condition relative to that obtained for respective positive controls (max. LDH release). Error bars represent ± SD of the measurement where $n = 3$.

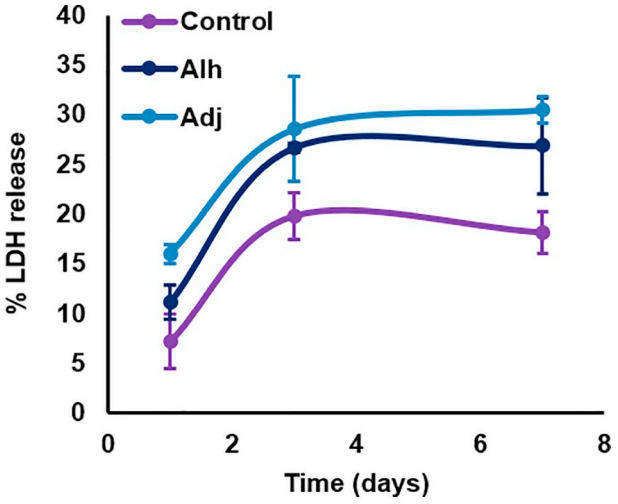

Fig. 7. LDH release (%) induced in untreated and adjuvant-treated samples relative to that obtained for respective positive controls (max. LDH release) over a period of seven days post exposure (control, Alh and Adj – purple, blue and green series respectively). Error bars represent ± SD of the measurement where $n = 3$. (For interpretation of the references to colour in this figure legend, the reader is referred to the web version of this article.)

this particular transition that may account for the decrease in Al and DAPI positive cells observed on day 7 of the experiment vs. that of the preceding time point. However, while it must be emphasised that there are differences between primary MDMs and those derived from cell lines [47,51,52], THP-1 macrophages provide both a stable and appropriate model to monitor the impact of ABA phagocytosis in vitro.

Neither form of ABA caused specific interference with the results generated by the LDH assay at the concentrations used herein (data not shown). In fact, this method has been used to successfully evaluate the viability of cells exposed to higher concentrations of AH (1 mg/mL Al) without significant artefacts being explicitly encountered [53]. Our decision to modify the assay through the use of ABA-spiked maximum LDH controls was predicated upon the notion that micro-particulates can inactivate and adsorb enzymes released by dying cells, leading to the generation of false negative readings [54]. Other limitations of this assay include the inherent LDH activity of serum containing culture medium [55]; however, this was accounted for using medium only controls as absorbance values were not exceptionally high. The complementary measurement of metabolic activity, despite its popularity in this context, was not attempted owing to the documented influence of ABAs on mitochondrial function [56]. LDH data was instead paired with direct dead cell labelling (DAPI staining) in order to evaluate the impact of ABAs upon individual cells as well as the total population. In conjunction, these methods allowed the relationship between particle recognition, uptake and viability to be reliably elucidated.

Aluminium particulates were observed both within the cytoplasmic space and at the cellular margin of macrophages at junctures as early as 3 h post exposure, which is consistent with the size distribution previously determined for these species in R10 medium (*ca* 1 μm) [21]. Particulate loading was extensive & heterogenous in nature and the degree of cytosolic burden typically observed in individual cells was moderate to high 24–72 h following treatment. The latter was more pronounced in cells exhibiting rounded morphologies, a phenomenon perhaps attributed to their lower relative cytoplasmic volume. Previous communications have inferred that AH is more avidly engulfed by immature phagocytes [21]; however, qualitative assessment of ABA uptake herein revealed no observable differences in cellular loading between adjuvant species at any point during experiments. Furthermore, our results confirm that macrophages both interact with and internalise ABAs in situ, which is consistent with trends observed by others in vivo [14,34,35,38–41].

The heightened and prevalent incidence of ABAs within THP-1 macrophages did not necessarily correlate with a concomitant increase in cell death either on an individual (DAPI staining) or widespread basis (LDH assay). Early indications did suggest that AP caused a small but significant reduction in total cell viability relative to untreated controls; however, this was only apparent on day 1 of the experiment. While the sensitivity of their progenitors to small amounts of AP has already been demonstrated [21], macrophages appear more resilient in this context, conceivably due to their prominent role in pathogenic clearance and host defence [57]. Our results are also consistent with those

demonstrating that low doses of ABAs increased the life-span of murine macrophages in the absence of additional stimulating factors, enhancing DNA synthesis through undisclosed pathways [42]. However, higher concentrations of Al (1 mg/mL) administered in the form of AH prompted a significant elevation in the expiration of peritoneal macrophages in vitro (*ca* 50%) only 48 h after initial exposure, although this did not seem to be directly related to particle entrapment [53]. In combination, these findings indicate that ABAs may exert their influence upon immune cells in a concentration-dependent biphasic manner i.e. stimulatory at low and inhibitory at high concentrations. They also imply that an excess of ABAs in the extracellular milieu may contribute to the cell death observed when high concentrations are introduced; however, this hypothesis has yet to be experimentally confirmed.

The relatively low incidence of cellular death directly observed in populations heavily laden with particles also demonstrates that a large proportion of THP-1 macrophages are extremely tolerant to large cytosolic burdens of ABAs. It is thus apparent that ABA-mediated cytotoxicity may be somewhat independent of particle uptake or that the majority of cells have diminished susceptibility to particulate induced toxicity. Crystalline ABAs, in particular, demonstrate membranolytic activity including the ability to disrupt lysosomes [58–61], a precursor to immune cell necrosis and potent stimulus for the induction of humoral responses [61]. Events of this nature, however, appear to be relatively scarce within host muscle tissue post immunisation and restricted to *ca* 2.5% of the local population in the short term [62]. Indeed, the uncontrolled and widespread death of APCs upon contact with ABAs in vivo appears counterintuitive with regards to the transference of antigen-adjuvant complexes to the draining lymph nodes, a process reportedly essential for vaccine priming and the generation of robust immunological responses [20].

In conclusion, this study is the first direct demonstration that the cellular internalisation of ABAs by macrophages does not necessarily induce significant levels of cytotoxicity. As a result, the majority of macrophages remained viable for up to 7 days post treatment. While such trends also need to be confirmed using primary MDMs, the longevity of these cells in vitro indirectly supports their role in cell-mediated particulate trafficking to the draining lymph nodes, which reportedly initially peaks around 4–7 days after vaccination [38,40]. Clarification of the precise mechanisms through which ABAs perpetuate the survival of immunocompetent cells is required in order to better understand the risks associated with their biological administration in predisposed individuals, including the slow CCL2-dependent dissemination of particles to the brain [38,40,41].

Funding

ES is a Children's Medical Safety Research Institute (CMSRI) Research Fellow.

Author contributions

Conceptualization; ES, MM, CE; Funding acquisition; CE; Investigation; ES, MM. Writing - original draft; ES; Writing - review & editing; ES, MM, CE.

Declaration of competing interest

The authors have no conflicts of interest to disclose.

Acknowledgements

Dr. David Mazzocchi-Jones is thanked for allowing access to cell culture facilities. Dr. Mirna Mourtada Maarabouni is thanked for allowing access to EVOS live cell imaging system.

Appendix A. Supplementary data

Supplementary data to this article can be found online at https://doi.org/10.1016/j.jinorgbio.2019.110915.

References

[1] H. Hogenesch, Mechanism of immunopotentiation and safety of aluminum adjuvants, Front. Immunol. 3 (2013) 406.
[2] T.R. Ghimire, The mechanisms of action of vaccines containing aluminum adjuvants: an in vitro vs in vivo paradigm, SpringerPlus 4 (2015) 181.
[3] J.L. Grun, P.H. Maurer, Different T helper cell subsets elicited in mice utilizing two different adjuvant vehicles: the role of endogenous interlukin-1 in proliferative responses, Cell. Immunol. 121 (1989) 134–145.
[4] J.M. Brewer, M. Conacher, A. Satoskar, H. Bluethmann, J. Alexander, In interleukin-4-deficient mice, alum not only generates T helper 1 responses equivalent to Freund's complete adjuvant, but continues to induce T helper 2 cytokine production, Eur. J. Immunol. 26 (1996) 2062–2066.
[5] M.B. Jordan, D.M. Mills, J. Kappler, P. Marrack, J.C. Cambier, Promotion of B cell immune responses via an alum-induced myeloid cell population, Science 304 (2004) 1808–1810.
[6] K.S. Korsholm, R.V. Petersen, E.M. Agger, P. Andersen, T-helper 1 and T-helper 2 adjuvants induce distinct differences in the magnitude, quality and kinetics of the early inflammatory response at the site of injection, Immunology 129 (1) (2010) 75–86.
[7] R.K. Gherardi, M. Coquet, P. Cherin, L. Belec, P. Moretto, P.A. Dreyfus, J.F. Pellissier, P. Chariot, F.J. Authier, Macrophagic myofasciitis lesions assess long-term persistence of vaccine-derived aluminium hydroxide in muscle, Brain 124 (Pt 9) (2001) 1821–1831.
[8] R.K. Gherardi, F.J. Authier, Aluminum inclusion macrophagic myofasciitis: a recently identified condition, Immunol. Allergy Clin. N. Am. 23 (4) (2003) 699–712.
[9] M. Rigolet, J. Aouizerate, M. Couette, N. Ragunathan-Thangarajah, M. Aoun-Sebaiti, R.K. Gherardi, J. Cadusseau, F.J. Authier, Clinical features in patients with long-lasting macrophagic myofasciitis, Front. Neurol. 5 (2014) 230.
[10] M. Shingde, J. Hughes, R. Boadle, E.J. Wills, R. Pamphlett, Macrophagic myofasciitis associated with vaccine-derived aluminium, Med. J. Aust. 183 (3) (2005) 145–146.
[11] S.J. Seeber, J.L. White, S.L. Hem, Solubilization of aluminum-containing adjuvants by constituents of interstitial fluid, Parenter. Sci. Technol. 45 (1991) 156–159.
[12] S.L. Hem, Elimination of aluminum adjuvants, Vaccine 20 (Suppl. 3) (2002) S40–S43.
[13] R.E. Flarend, S.L. Hem, J.L. White, D. Elmore, M.A. Suckow, A.C. Rudy, E.A. Dandashli, In vivo absorption of aluminum-containing vaccine adjuvants using 26Al, Vaccine 15 (1997) 1314–1318.
[14] F. Verdier, R. Burnett, C. Michelet-Habchi, P. Moretto, F. Fievet-Groyne, E. Sauzeat, Aluminium assay and evaluation of the local reaction at several time points after intramuscular administration of aluminium containing vaccines in the Cynomolgus monkey, Vaccine 23 (11) (2005) 1359–1367.
[15] M.W. Munks, A.S. McKee, M.K. Macleod, R.L. Powell, J.L. Degen, N.A. Reisdorph, J.W. Kappler, P. Marrack, Aluminum adjuvants elicit fibrin-dependent extracellular traps in vivo, Blood 116 (24) (2010) 5191–5199.
[16] J. Stephen, H.E. Scales, R.A. Benson, D. Erben, P. Garside, J.M. Brewer, Neutrophil swarming and extracellular trap formation play a significant role in alum adjuvant activity, NPJ Vaccines 2 (1) (2017).
[17] S. Hutchison, R.A. Benson, V.B. Gibson, A.H. Pollock, P. Garside, J.M. Brewer, Antigen depot is not required for alum adjuvanticity, FASEB J. 26 (3) (2012) 1272–1279.
[18] C.J. Chen, H. Kono, D. Golenbock, G. Reed, S. Akira, K.L. Rock, Identification of a key pathway required for the sterile inflammatory response triggered by dying cells, Nat. Med. 13 (2007) 851–856.
[19] H. Kono, D. Karmarkar, Y. Iwakura, K.L. Rock, Identification of the cellular sensor that stimulates the inflammatory response to sterile cell death, J. Immunol. 184 (2010) 4470–4478.
[20] F. Liang, G. Lindgren, K.J. Sandgren, E.A. Thompson, J.R. Francica, A. Seubert, E. De Gregorio, S. Barnett, D.T. O'Hagan, N.J. Sullivan, R.A. Koup, R.A. Seder, K. Loré, Vaccine priming is restricted to draining lymph nodes and controlled by adjuvant-mediated antigen uptake, Sci. Transl. Med. 9 (393) (2017) (pii: eaal2094).
[21] M. Mold, E. Shardlow, C. Exley, Insight into the cellular fate and toxicity of aluminium adjuvants used in clinically approved human vaccinations, Sci. Rep. 6 (2016) 31578.
[22] J.A. Champion, A. Walker, S. Mitragotri, Role of particle size in phagocytosis of polymeric microspheres, Pharm. Res. 25 (2008) 1815–1821.
[23] F. Lu, H. Hogenesch, Kinetics of the inflammatory response following intramuscular injection of aluminum adjuvant, Vaccine 31 (37) (2013) 3979–3986.
[24] M. Mold, H. Eriksson, P. Siesjo, A. Darabi, E. Shardlow, C. Exley, Unequivocal identification of intracellular aluminium adjuvant in a monocytic THP-1 cell line, Sci. Rep. 4 (1) (2014) 6287.
[25] M. Mold, M. Kumar, A. Mirza, E. Shardlow, C. Exley, Intracellular tracing of amyloid vaccines through direct fluorescent labelling, Sci. Rep. 5 8 (1) (2018) 2437.
[26] M. Ulanova, A. Tarkowski, M. Hahn-Zoric, L.A. Hanson, The common vaccine adjuvant aluminum hydroxide up-regulates accessory properties of human monocytes via an interleukin-4-dependent mechanism, Infect. Immun. 69 (2) (2001) 1151–1159.
[27] A. Seubert, E. Monaci, M. Pizza, D.T. O'Hagan, A. Wack, The adjuvants aluminum

hydroxide and MF59 induce monocyte and granulocyte chemoattractants and enhance monocyte differentiation toward dendritic cells, J. Immunol. 180 (8) (2008) 5402–5412.
[28] S. Kooijman, J. Brummelman, C.A.C.M. van Els, F. Marino, A.J.R. Heck, G.P.M. Mommen, B. Metz, G.F.A. Kersten, J.L.A. Pennings, H.D. Meiring, Novel identified aluminum hydroxide-induced pathways prove monocyte activation and pro-inflammatory preparedness, J. Proteome 175 (2018) 144–155.
[29] M. Kool, T. Soullié, M. van Nimwegen, M.A. Willart, F. Muskens, S. Jung, H.C. Hoogsteden, H. Hammad, B.N. Lambrecht, Alum adjuvant boosts adaptive immunity by inducing uric acid and activating inflammatory dendritic cells, J. Exp. Med. 205 (4) (2008) 869–882.
[30] G.L. Morefield, A. Sokolovska, D. Jiang, H. HogenEsch, J.P. Robinson, S.L. Hem, Role of aluminum-containing adjuvants in antigen internalization by dendritic cells in vitro, Vaccine 23 (2005) 1588–1595.
[31] A. Sokolovska, S.L. Hem, H. HogenEsch, Activation of dendritic cells and induction of CD4(+) T cell differentiation by aluminum-containing adjuvants, Vaccine 25 (2007) 4575–4585.
[32] T.R. Ghimire, R.A. Benson, P. Garside, J.M. Brewer, Alum increases antigen uptake, reduces antigen degradation and sustains antigen presentation by DCs in vitro, Immunol. Lett. 147 (2012) 55–62.
[33] A.S. McKee, M.W. Munks, M.K. MacLeod, C.J. Fleenor, N. Van Rooijen, J.W. Kappler, P. Marrack, Alum induces innate immune responses through macrophage and mast cell sensors, but these sensors are not required for alum to act as an adjuvant for specific immunity, J. Immunol. 183 (2009) 4403–4414.
[34] A.C. Rimaniol, G. Gras, F. Verdier, F. Capel, V.B. Grigoriev, F. Porcheray, E. Sauzeat, J.G. Fournier, P. Clayette, C.A. Siegrist, D. Dormont, Aluminum hydroxide adjuvant induces macrophage differentiation towards a specialized antigen-presenting cell type, Vaccine 22 (23–24) (2004) 3127–3135.
[35] A.C. Rimaniol, G. Gras, P. Clayette, In vitro interactions between macrophages and aluminum-containing adjuvants, Vaccine 25 (37–38) (2007) 6784–6792.
[36] X. Li, S. Hufnagel, H. Xu, S.A. Valdes, S.G. Thakkar, Z. Cui, H. Celio, Aluminum (oxy)hydroxide nanosticks synthesized in bicontinuous reverse microemulsion have potent vaccine adjuvant activity, ACS Appl. Mater. Interfaces 9 (27) (2017) 22893–22901.
[37] X. Li, A.M. Aldayel, Z. Cui, Aluminum hydroxide nanoparticles show a stronger vaccine adjuvant activity than traditional aluminium hydroxide microparticles, J. Control. Release 173 (2014) 148–157.
[38] Z. Khan, C. Combadiere, F.J. Authier, V. Itier, F. Lux, C. Exley, M. Mahrouf-Yorgov, X. Decrouy, P. Moretto, O. Tillement, R.K. Gherardi, J. Cadusseau, Slow CCL2-dependent translocation of biopersistent particles from muscle to brain, BMC Med. 11 (2013) 99.
[39] J. Asín, J. Molín, M. Pérez, P. Pinczowski, M. Gimeno, N. Navascués, A. Muniesa, I. de Blas, D. Lacasta, A. Fernández, L. de Pablo, M. Mold, C. Exley, D. de Andrés, R. Reina, L. Luján, Granulomas following subcutaneous injection with aluminum adjuvant-containing products in sheep, Vet. Pathol. 56 (3) (2019) 418–428.
[40] H. Eidi, M.O. David, G. Crépeaux, L. Henry, V. Joshi, M.H. Berger, M. Sennour, J. Cadusseau, R.K. Gherardi, P.A. Curmi, Fluorescent nanodiamonds as a relevant tag for the assessment of alum adjuvant particle biodisposition, BMC Med. 13 (2015) 144.
[41] G. Crépeaux, H. Eidi, M.O. David, E. Tzavara, B. Giros, C. Exley, P.A. Curmi, C.A. Shaw, R.K. Gherardi, J. Cadusseau, Highly delayed systemic translocation of aluminum-based adjuvant in CD1 mice following intramuscular injections, J. Inorg. Biochem. 152 (2015) 199–205.
[42] J.A. Hamilton, R. Byrne, G. Whitty, Particulate adjuvants can induce macrophage survival, DNA synthesis, and a synergistic proliferative response to GM-CSF and CSF-1, J. Leukoc. Biol. 67 (2) (2000) 226–232.
[43] S. Tsuchiya, M. Yamabe, Y. Yamaguchi, Y. Kobayashi, T. Konno, K. Tada, Establishment and characterization of a human acute monocytic leukemia cell line (THP-1), Int. J. Cancer 26 (1980) 171–176.
[44] D.J. Hydes, P.S. Liss, Fluorimetric method for determination of low concentrations of dissolved aluminum in natural-waters, Analyst 101 (1976) 922–931.
[45] J.L. Ren, J. Zhang, J.Q. Luo, X.K. Pei, Z.X. Jiang, Improved fluorimetric determination of dissolved aluminium by micelle-enhanced lumogallion complex in natural waters, Analyst 126 (2001) 698–702.
[46] N.W. Baylor, W. Egan, P. Richman, Aluminium salts in vaccines – US perspective, Vaccine 29 (2012) S18–S23.
[47] M. Daigneault, J.A. Preston, H.M. Marriott, M.K. Whyte, D.H. Dockrell, The identification of markers of macrophage differentiation in PMA-stimulated THP-1 cells and monocyte-derived macrophages, PLoS One 5 (2010) e8668.
[48] W. Chanput, J.J. Mes, H.J. Wichers, THP-1 cell line: an in vitro cell model for immune modulation approach, Int. Immunopharmacol. 23 (2014) 37–45.
[49] H. Schwende, E. Fitzke, P. Ambs, P. Dieter, Differences in the state of differentiation of THP-1 cells induced by phorbol ester and 1,25-dihydroxyvitamin D3, J. Leukoc. Biol. 59 (1996) 555–561.
[50] M.E. Lund, J. To, B.A. O'Brien, S. Donnelly, The choice of phorbol 12-myristate 13-acetate differentiation protocol influences the response of THP-1 macrophages to a pro-inflammatory stimulus, J. Immunol. Methods 430 (2016) 64–70.
[51] T. Starr, T.J. Bauler, P. Malik-Kale, O. Steele-Mortimer, The phorbol 12-myristate-13-acetate differentiation protocol is critical to the interaction of THP-1 macrophages with Salmonella typhimurium, PLoS One 13 (3) (2018) e0193601.
[52] S. Tedesco, F. De Majo, J. Kim, A. Trenti, L. Trevisi, G.P. Fadini, C. Bolego, P.W. Zandstra, A. Cignarella, L. Vitiello, Convenience versus biological significance: are PMA-differentiated THP-1 cells a reliable substitute for blood-derived macrophages when studying in vitro polarization? Front. Pharmacol. 9 (2018) 71.
[53] N. Goto, H. Kato, J. Maeyama, K. Eto, S. Yoshihara, Studies on the toxicities of aluminium hydroxide and calcium phosphate as immunological adjuvants for vaccines, Vaccine 11 (9) (1993) 914–918.
[54] A.L. Holder, R. Goth-Goldstein, D. Lucas, C.P. Koshland, Particle-induced artifacts in the MTT and LDH viability assays, Chem. Res. Toxicol. 25 (9) (2012) 1885–1892.
[55] O.S. Aslantürk, In vitro cytotoxicity and cell viability assays: principles, advantages, and disadvantages, in: M.L. Larramendy, S. Soloneski (Eds.), Genotoxicity - a Predictable Risk to Our Actual World, IntechOpen, 2018.
[56] L. Ohlsson, C. Exley, A. Darabi, E. Sandén, P. Siesjö, H. Eriksson, Aluminium based adjuvants and their effects on mitochondria and lysosomes of phagocytosing cells, J. Inorg. Biochem. 128 (2013) 229–236.
[57] D.M. Mosser, J.P. Edwards, Exploring the full spectrum of macrophage activation, Nat. Rev. Immunol. 8 (12) (2008) 958–969.
[58] T.B. Ruwona, H. Xu, X. Li, A.N. Taylor, Y.C. Shi, Z. Cui, Toward understanding the mechanism underlying the strong adjuvant activity of aluminum salt nanoparticles, Vaccine 34 (27) (2016) 3059–3067.
[59] H. Lima Jr., L.S. Jacobson, M.F. Goldberg, K. Chandran, F. Diaz-Griffero, M.P. Lisanti, J. Brojatsch, 2013. Role of lysosome rupture in controlling Nlrp3 signaling and necrotic cell death. Cell Cycle. 12(12), 1868-1678.
[60] F.A. Sharp, D. Ruane, B. Claass, E. Creagh, J. Harris, P. Malyala, M. Singh, D.T. O'Hagan, V. Pétrilli, J. Tschopp, L.A. O'Neill, E.C. Lavelle, Uptake of particulate vaccine adjuvants by dendritic cells activates the NALP3 inflammasome, Proc. Natl. Acad. Sci. U. S. A. 106 (3) (2009) 870–875.
[61] V. Hornung, F. Bauernfeind, A. Halle, E.O. Samstad, H. Kono, K.L. Rock, K.A. Fitzgerald, E. Latz, Silica crystals and aluminum salts activate the NALP3 inflammasome through phagosomal destabilization, Nat. Immunol. 9 (8) (2008) 847–856.
[62] T. Marichal, K. Ohata, D. Bedoret, C. Mesnil, C. Sabatel, K. Kobiyama, P. Lekeux, C. Coban, S. Akira, K.J. Ishii, F. Bureau, C.J. Desmet, DNA released from dying host cells mediates aluminum adjuvant activity, Nat. Med. 17 (8) (2011) 996–1002.